Shi, Z., Lai, D., and Chen, Q. 2020. "Performance evaluation and design guide for a coupled displacement-ventilation and passive-chilled-beam system," *Energy and Buildings*, 208:109654.

Performance Evaluation and Design Guide for a Coupled Displacement-Ventilation and Passive-Chilled-Beam System

Zhu Shi[1], Dayi Lai[2], Qingyan Chen[1]*

[1]School of Mechanical Engineering, Purdue University, West Lafayette, IN 47907, USA

[2]Department of Architecture, School of Design, Shanghai Jiao Tong University, Shanghai 200240, China

*Phone: (765) 496-7562, Fax: (765) 496-0539, Email: yanchen@purdue.edu

Nomenclature

A	Area of room	S_{vapor}	Water vapor generation rate
C	Contaminant concentration	S_{ϕ}	Source term in transport equation
$C_{1.1m}$	Contaminant concentration at head level (sitting person)	T	Dry bulb temperature
C_h	Contaminant concentration at a specific sampling height	$T_{0.1\mathrm{m}}$	Air temperature at ankle level
C_e	Contaminant concentration at exhaust	T_{dp}	Dew point
C_p	Specific heat at constant pressure	T_e	Temperature of exhaust air
C_s	Contaminant concentration at supply	T_{room}	Room air temperature
C^*	Normalized contaminant concentration	T_s	Temperature of supply air
h	Height of PCB	T_{sp}	Temperature setpoint
h_0	Reference height of PCB	$T_{w,s}$	Chilled water supply temperature
H	Room height	t	Time
H^*	Normalized height	u_i	Velocity in i direction
n	Air change per hour	U	Velocity magnitude
L	Length of PCB	U^*	Normalized velocity
$\dot{m}_{air}$	Air mass flow rate	V_f	Required outdoor airflow rate
$\dot{m}_{inf}$	Air mass flow rate through infiltration	V_h	Required airflow rate to maintain thermal comfort requirement
N	Number of occupants	W	Width of PCB
q	Chilled water flow rate	x	Outdoor air ratio
Q_{ex}	Cooling loads from exterior	x_i	Coordinate in i direction
Q_l	Cooling loads from lighting	ΔT_{ha}	Temperature difference between head and feet
Q_{oz}	Cooling loads in occupied zone	θ_f	Dimensionless air temperature near floor
Q_{PCB}	Cooling load removed by PCB	η	Percentage of cooling load removed by PCB
Q_t	Total cooling load	ρ	Density

R_a	Outdoor air rate per unit floor area	Φ	Relative humidity
R_p	Outdoor air rate per occupant	ω	Absolute humidity
s	Water vapor generation rate per occupant		

Abstract

Displacement ventilation (DV) can provide good air quality to indoor spaces while saving energy. Research has shown that, since the supply air temperature in DV cannot be very low, its capability to remove a high cooling load is limited. Previous studies found that passive chilled beams (PCBs) could be coupled with DV to enhance the cooling capability of the latter and reduce the vertical temperature gradient. However, PCBs also recirculate airborne contaminants downward, reducing the air quality in the occupied zone. Therefore, it is essential to design a DV-PCB system for optimal thermal comfort and indoor air quality. This study established a database of 70 cases that include four typical types of indoor spaces with DV-PCB systems and developed mathematical models for predicting the thermal and ventilation performance of a DV-PCB system based on various design parameters. With the models, this investigation then proposed a step-by-step procedure for designing a DV-PCB system to create a thermally comfortable and healthy indoor environment without causing condensation on the chilled beams. Moreover, a user-friendly design interface was developed that can be used by engineers to make design decisions conveniently.

Key words

Mathematical model, Thermal comfort, Indoor air quality, Ventilation performance, Database

1. Introduction

Previous studies showed that displacement ventilation (DV) can provide good indoor air quality while saving energy [1, 2, 3]. Because of these advantages, DV has been commonly used in Nordic countries since the 1970s, and, more recently, in the United States [4, 5]. However, Rees and Haves [6] and Alain et al. [7] have also indicated that a DV system has limited capability to remove high cooling loads. Since the DV system supplies air to the occupied zone directly, the temperature of its supply air should not be too low. In addition, the use of DV in an indoor space with a high cooling load can produce a large temperature gradient in the occupied zone, which is not conducive to thermal comfort. According to several studies [8, 9, 10], a DV system alone is capable of providing acceptable comfort only if the corresponding cooling load is less than 40 W/m^2. With the increasing use of electrical equipment in today's buildings, it is necessary to seek improvements to DV, so that a thermally comfortable and healthy indoor environment can be achieved.

Several prior studies investigated using chilled ceiling panels in a DV system to enhance cooling efficiency [11, 12, 13]. For example, Schiavon et al. [12] conducted experiments in a typical U.S.

interior office with chilled ceiling panels removing up to 73W/m^2 of cooling load, and demonstrated that temperature stratification decreased as a larger portion of load was removed by chilled ceiling. Rees and Haves [6] measured the air temperature distribution in a room (72W/m^2) with combined DV and chilled ceiling system, which reported an almost linear temperature gradient of 3 K/m between 0.4 m to 1.0 m height. Ghali et al. [14] and Bahman et al. [15] further compared the energy consumptions between the combined system and an all-air system over a cooling season, and concluded that this combined system led to an energy saving of more than 20%. Although it was found that the combined system could remove a large cooling load while being energy efficient, studies [6, 16] also showed that, when chilled ceiling was used to handle too much cooling load, it could destroy the stratified displacement airflow pattern which results in mixed contaminant distribution. In addition, there is a considerable condensation risk on the surface of the chilled ceiling panels [17]. Moreover, in a chilled ceiling system, metal panels are mounted on the ceiling with chilled water pipes embedded within them, which led to a very high first cost [18, 19]. Meanwhile, passive chilled beams (PCBs), which cool ambient air via chilled water pipes inside the beam unit and are suspended near the ceiling, can remove a large cooling load [20, 21]. According to Nelson [22], the indoor airflow pattern and heat transfer mechanism of PCBs were significantly different from those in chilled ceiling systems. Fredriksson and Sandberg [23] tested the cooling performance of PCBs under various loads and found that PCBs were able to remove up to 80% of cooling loads in a room. Shi et al. [24] used experimental and simulation methods to investigate the impact of PCB on the temperature distribution developed by DV and found that PCB greatly reduced the vertical temperature gradient, which improved thermal comfort. Compared with the chilled ceiling system, a PCB system has a greater cooling output, better flexibility and lower first cost [18]. Hence, the PCB should be coupled with DV to remove a large cooling load. However, PCB also created a downward air jet as reported by many studies [20, 24, 25]. Fredriksson et al. [25] demonstrated by experiments that this downward jet had similar behavior with two-dimensional jet and the maximum measured velocity was 0.28 m/s. Shi et al. [24] and Shan and Rim [26] showed that this cool jet recirculates airborne contaminants near the ceiling downward into the occupied zone, which may weaken the contaminant stratification developed by DV. Therefore, in order to achieve optimal thermal comfort and indoor air quality with the coupled DV-PCB system, it is imperative to quantitatively evaluate this system and develop a suitable design guide.

In addition, a major concern in the design of any air-water system is the risk of condensation on chilled surfaces [27, 28, 29]. If it is not well controlled, condensation can continually form and drip onto occupants or objects in the occupied zone. More seriously, it may lead to mold growth, which can escalate to an air quality problem [30, 31]. It is critical that strategies are implemented in the design phase to prevent condensation.

To guide the design of HVAC systems, both experimental and computational fluid dynamics (CFD) methods have been used in prior studies [32, 33]. These methods are normally time-consuming, and the experimental or computational tools are not always available to designers. However, the

methods provide valuable information about air temperature, air velocity and contaminant concentration in indoor spaces, and this data can help us understand the effects of various design parameters on the performance of an HVAC system. Moreover, the information can be used to develop simple mathematical models that quantify the thermal and ventilation performance of the coupled DV-PCB system. The models can then be used easily by engineers to judge the applicability of the system and to determine design parameters.

To develop the mathematical models, this investigation first performed a literature survey and determined ranges of key geometric parameters and thermal conditions for four common indoor spaces: classrooms, offices, industrial workshops and restaurants. Based on this survey, a validated CFD model was used to simulate and quantify the thermal and ventilation performance for 70 DV-PCB cases that encompassed wide range of design parameters. By using these cases as a database, this investigation developed simple mathematical models for predicting the temperature gradient and ventilation effectiveness at a given set of design parameters. Finally, a guide was developed to provide a step-by-step procedure for designing a DV-PCB system that meets thermal and ventilation requirements without the risk of condensation.

2. Research Methods

This investigation used a validated CFD model to establish a database of 70 DV-PCB cases for evaluating the thermal and ventilation performance of the system under various design conditions. The database was then employed to develop mathematical models for use by a designer in predicting the thermal and ventilation performance of DV-PCB coupled systems. This section describes the design of these cases, the parameters that were used to evaluate the thermal and ventilation performance, and the development of the mathematical models.

2.1 Indoor space layouts and ranges of design parameters

Fig. 1 shows the layouts of the four indoor spaces studied here: an office, a classroom, an industrial workshop and a restaurant. The office layout consists of regular cooling loads such as computers and lights, and it has a seating capacity of eight people. The classroom can hold 24 students and one instructor; this is the average classroom size in the US [34, 35]. The industrial workshop has a large floor area with high-power equipment on the tables in uniform distribution. The restaurant layout includes a combination of round, square and long tables as well as partitions, to simulate a typical dining space. In all cases, the locations and number of the PCBs were decided so that no occupants were right below PCB (for avoiding draft), every occupant had at least one PCB that was nearby for cooling, PCBs did not cross over with overhead lighting and that PCBs were evenly distributed near the ceiling to ensure they could cool the rooms uniformly. Air supply inlets were determined so that they were uniformly located at lower part of vertical walls for providing air to occupied zone from different directions. In addition, for minimizing the draft to the occupants, air inlets were not placed right in front of any of them.

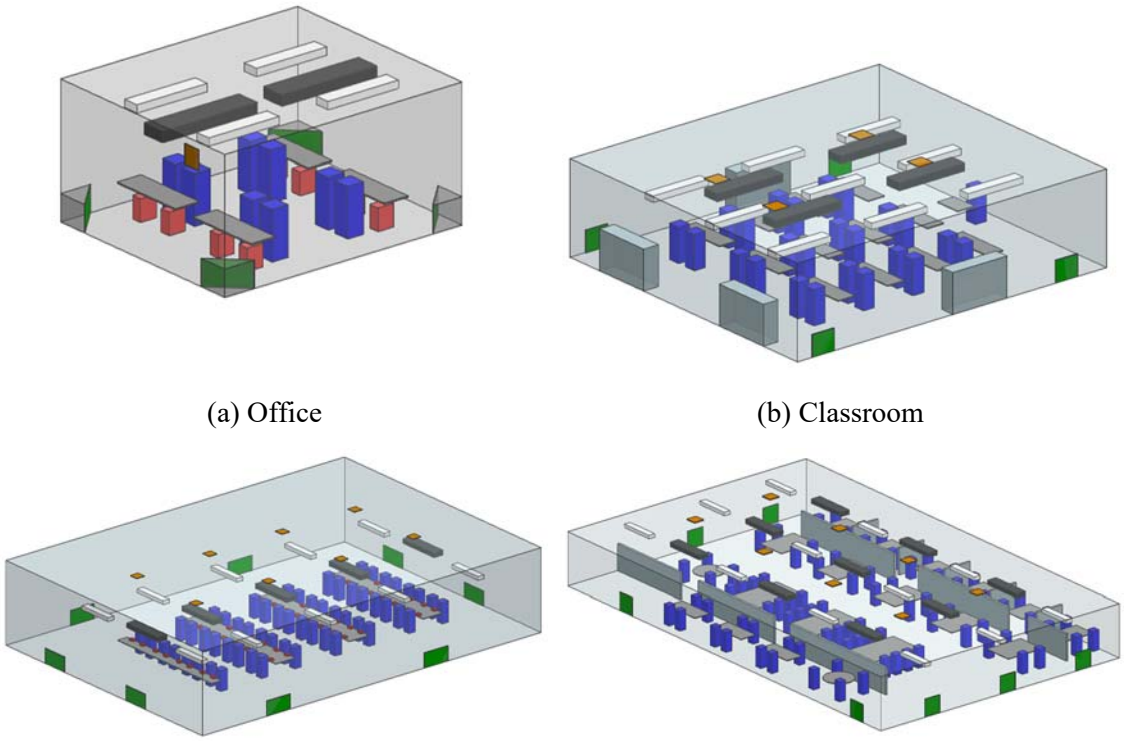

(a) Office (b) Classroom

(c) Industrial workshop (d) Restaurant

Fig. 1 Layouts of four indoor spaces in this study

(Legend: green – diffusers; blue – occupants; brown – exhausts; red – PCs and other electrical devices; white – lights; grey – tables and closets; black – PCBs)

It was critical to ensure that the design parameters used in these cases were within reasonable ranges. This investigation conducted a literature survey to determine these ranges. Table 1 lists the height ranges of the four indoor spaces, which were obtained from New York State DOH [36], US GSA [37] and Hu et al. [38]. Also listed in Table 1 are the ranges of the cooling loads. This study split cooling loads into three categories: Q_{oz} represents cooling loads in the occupied zone, such as occupants and equipment, Q_l stands for cooling loads from overhead lighting outside the occupied zone, and Q_{ex} represents exterior cooling loads that include transmitted solar radiation and heat from exterior surfaces and can enter both the occupied and unoccupied zones. Among these loads, the ranges for Q_l were determined from lighting levels recommended for the different indoor spaces by NOAO [39], while Q_{oz} and Q_{ex} were estimated according to ASHRAE Handbook [40] and ASHRAE [41]. The air change rate in an indoor space can vary, but it must be larger than $\left(R_a \times A + R_p \times N\right)$ to meet the minimum outdoor air requirement [42], where R_a, R_p, A, and N represent the outdoor air rate per unit floor area, outdoor air rate per occupant, floor area, and number of occupants, respectively. Previous research [43] showed that PCBs could

remove as much as 80% of the cooling load, and therefore this investigation used 80% as the upper bound for η in these cases. The details of each case are presented in Section 3.1.

Table 1. Room dimensions and ranges of parameters used for the four indoor spaces

		Office	Classroom	Workshop	Restaurant
Floor surface area, A (m^2)		31	101	320	410
Height, H (m)		2.4 - 3.5	2.7 - 3.8	3 - 5	2.7 - 3.5
Loads (W/m^2)	Occupied zone, Q_{oz}	5 - 50	5 - 25	10 - 35	5 - 25
	Lighting, Q_l	0 - 12.5	0 - 10	0 - 15	0 - 10
	Exterior, Q_{ex}	0 - 20	0 - 25	0 - 25	0 - 25
n (ACH)		3 -7, and resulting air rate should be greater than $\left(R_a \times A + R_p \times N\right)$			
Percentage of load removed by PCB, η		0 - 80%			

2.2 CFD modeling of indoor airflow and contaminant transport

This study employed a CFD model that was developed and validated by Shi et al. [24] to predict the airflow and contaminant transport in indoor spaces. With the use of the re-normalization group (RNG) k-ε turbulence model [44], which was recommended by Zhang and Chen [45] for simulating indoor airflow, this CFD model numerically solves mean air parameters through the following transport equation:

$$\rho\frac{\partial\langle\phi\rangle}{\partial t}+\rho\langle u_i\rangle\frac{\partial\langle\phi\rangle}{\partial x_i}-\frac{\partial}{\partial x_i}\left[\Gamma_{\phi,eff}\frac{\partial\langle\phi\rangle}{\partial x_i}\right]=S_\phi \quad (1)$$

where ϕ represents scalar terms (velocity components, turbulent kinetic energy, turbulent dissipation rate, energy and contaminant concentration in this study), S_ϕ is the source term, and $\Gamma_{\phi,eff}$ is the effective diffusion coefficient of scalar ϕ.

In the CFD model, non-slip boundary conditions ("walls") were used for internal surfaces including occupants, tables, partitions and vertical walls. Each PCB was modeled as an energy sink, whose energy absorption rate was calculated via dividing its heat removal rate by the corresponding volume. To account for the air density variation due to temperature difference, this research adopted Boussinesq model, which was shown to be accurate when the density difference was small [46]. To capture the large temperature gradient near heated surfaces while also properly discretizing the relatively complicated interior structure of computational domain, this study used structured mesh (inflation layers) in regions near surfaces and unstructured mesh in the interior region. Grid independence study was performed to make sure the grid size was appropriate for further investigation. This investigation used the ANSYS Fluent program [46] to perform the numerical simulations. SIMPLE (semi-implicit method for pressure-linked equations) scheme was used for

the pressure-velocity coupling and second-order spatial discretization method was used for velocity, turbulent kinetic energy, turbulent dissipation rate, energy and contaminant concentration terms. Infiltration was assumed to be marginal and was not modeled in the CFD simulations since many modern buildings implemented enhanced sealing technologies.

Fig. 2 compares the simulated airflow velocity, air temperature and tracer gas (SF_6) concentration with the measurement data in one of the measured cases. This case had an office layout with a cooling load of 90W/m^2. Heated sources included dummies (in yellow color), personal computers (in brown color), metal heated boxes (in pink color) and lights (near ceiling and not shown in Fig. 2). Dimension of each piece of PCB was $2.94m \times 0.43m \times 0.12m$. Due to limitation of space, the figures show the validation results on only one representative location at the center of room. The comparison shows that the results from CFD simulations were reasonably accurate. Hence, the model was used for further investigation. More details about this CFD model can be found in Shi et al. [24].

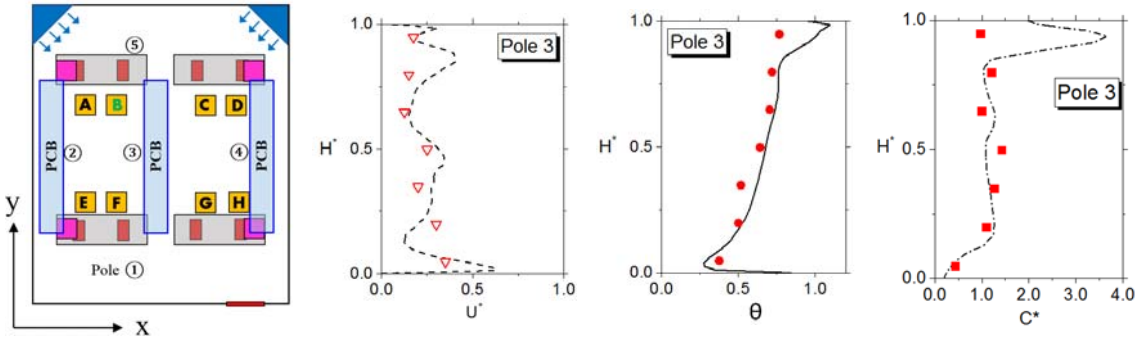

(a) Room layout (b) Velocity (c) Temperature (d) Tracer gas concentration

Fig. 2 Comparison of simulation and experimental results in a representative case ($U^* = U/U_s$, U_s=0.2 m/s; $\theta = (T - T_s)/(T_e - T_s)$; $C^* = (C - C_s)/(C_e - C_s)$; H*=z/H. Line: simulation; Symbol: measurement.)

2.3 Indices for evaluating thermal comfort and ventilation performance

To quantitatively appraise thermal and ventilation performance for a DV-PCB system, this investigation used the vertical temperature difference between the head and ankle levels of a seated person, ΔT_{ha}, and ventilation effectiveness, VE. The ΔT_{ha} is defined as:

$$\Delta T_{ha} = T_{1.1\mathrm{m}} - T_{0.1\mathrm{m}} \quad (2)$$

where $T_{1.1m}$ represents the air temperature at head level for a seated occupant, and $T_{0.1m}$ represents the air temperature at ankle level. According to ASHRAE [41], ΔT_{ha} should be lower than 3 K to prevent thermal discomfort due to the vertical temperature difference. This study defined VE as:

$$VE = \frac{C_e - C_s}{C_{1.1m} - C_s} \tag{3}$$

where $C_{1.1m}$, C_e and C_s are contaminant concentrations at head level for a seated occupant, at the exhaust, and at the supply, respectively. ASHRAE [42] recommends the use of empirical values VE = 1.2 for a DV system and VE = 1 for a mixed ventilation system. However, previous studies [1, 23] showed that the actual VE is affected by multiple parameters. In a coupled DV-PCB system, VE not only indicates the extent to which contaminant stratification is destroyed, but is also critical in determining the required outdoor airflow rate.

2.4 Development of mathematical models for ΔT_{ha} and VE

One objective of the present study was to develop mathematical models for determining ΔT_{ha} and VE, which are important criteria for engineers in designing a DV-PCB system. Previous studies showed that in a DV system, ΔT_{ha} and VE are both correlated with Q_{oz}, Q_l, Q_{ex}, n and H. As will be shown in Section 3.1, ΔT_{ha} and VE in a DV-PCB system were also dependent on η and ACH. Hence, in the coupled DV-PCB system, ΔT_{ha} should be expressed as:

$$\Delta T_{ha} = f\left(Q_{oz}, Q_l, Q_{ex}, n, H, A, \eta, \cdots\right) \tag{4}$$

Eq. (4) could further be expressed as:

$$\Delta T_{ha} = f_1\left(Q_{oz}, Q_{ex}, Q_l, Q_t, \mathrm{h}, \eta\right) f_2\left(Q_t, ACH, H, A, \eta\right) \tag{5}$$

Here, f_2 represents the temperature difference between the air exhaust and supply in the room:

$$f_2\left(Q_t, ACH, H, A, \eta\right) = T_e - T_s = \frac{(1-\eta)Q_t}{\rho C_p n A} \tag{6}$$

In Eq. (5), f_1 represents the ratio of the temperature difference in the occupied zone to the temperature difference between air near the floor and air near the ceiling. The f_1 can be evaluated in terms of the cooling load distribution:

$$f_1\left(Q_{oz}, Q_{ex}, Q_l, Q_t, \eta, h\right) = \frac{\sum_{i=oz,ex,l} \alpha_i Q_i - \beta Q_{PCB}}{(1-\eta)Q_t} \tag{7}$$

Similarly, VE should be expressed as:

$$VE = g\left(Q_{oz}, Q_l, Q_{ex}, n, H, A, \eta, \cdots\right) \tag{8}$$

This investigation used the database to determine the functions in Eqs. (7) and (8).

2.5 Two air handling systems that could be employed

Fig. 3 shows two possible air systems that can be employed in DV-PCB: a dedicated outdoor air system (DOAS) and an air recirculation system. The DOAS supplies 100% outdoor air to an indoor space through DV, while the air recirculation system mixes part of the return air with outdoor air to save energy. Both systems are commonly used, but since air recirculation system could recirculate part of moisture back to indoor space, the humidity ratios of the supply air in the two systems might be different. This research developed condensation strategies that could work for both system.

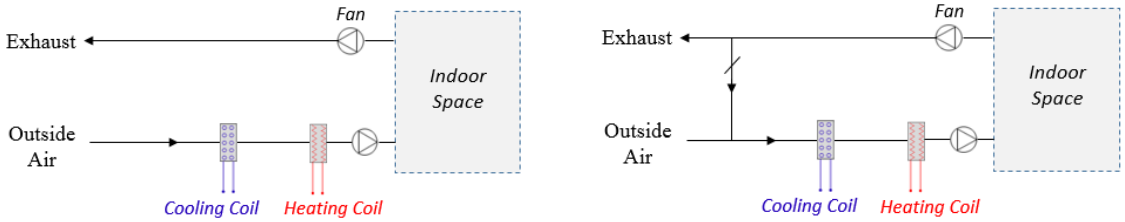

(a) DOAS (b) Air recirculation system

Fig. 3 Two possible air handling systems

2.6 Development of a user interface for design

The results in this study were further used to establish a five-step guide for designing a DV-PCB system. To make the guide more user friendly, a design tool was developed by incorporating the mathematical models and design procedure developed here. This study also included features that account for potential infiltration into the room. The design tool provides a straightforward design interface for use by engineers.

3. Results

This section first provides the specifications of the 70 cases in the database. With the results of these cases, this investigation examined the impact of key parameters on ΔT_{ha} and VE in a DV-PCB system and developed mathematical models to correlate ΔT_{ha} and VE with various design parameters. Strategies were also implemented to prevent condensation on the surface of the PCB cooling coil. Based on the mathematical models developed here, this study developed a guide and user interface for designing a DV-PCB system.

3.1 Case specifications and typical results

As shown in Table 2. the 70 cases in this investigation included 19 cases for the office layout, 17 for the classroom, 17 for the workshop and 17 for the restaurant. Contaminants were released from locations of occupants. For each layout, various combinations of design parameters were used. These parameters were changed one by one among the cases, which facilitated a sensitivity study

of the parameters' influence on ΔT_{ha} and VE. The parameters changed in each case are indicated by bold type in Table 2.

Table 2. Specifications of the 70 cases in the database

(a) Offices

Case #	H (m)	n (ACH)	Q_{oz} /A (W/m^2)	Q_l /A (W/m^2)	Q_{ex} /A (W/m^2)	Q_t /A (W/m^2)	η (-)	h (m)
OF.1	**2.75**	5	39.4	8.1	10.0	57.5	40%	2.51
OF.2	**3.35**	5	39.4	8.1	10.0	57.5	40%	2.51
OF.3	**3.05**	**3**	39.4	8.1	10.0	57.5	40%	2.51
OF.4	3.05	**5**	39.4	8.1	10.0	57.5	40%	2.51
OF.5	3.05	**7**	**39.4**	**8.1**	**10.0**	**57.5**	40%	2.51
OF.6	3.05	5	**12.2**	**6.1**	**0**	**18.2**	40%	2.51
OF.7	3.05	5	**24.0**	**6.1**	**0**	**30.0**	40%	2.51
OF.8	3.05	5	**43.6**	**8.1**	**10.0**	**61.7**	40%	2.51
OF.9	3.05	5	**49.1**	**12.1**	**10.0**	**71.2**	40%	2.51
OF.10	3.05	5	**49.1**	**12.1**	**30.0**	**91.2**	40%	2.51
OF.11	3.05	5	39.4	8.1	10.0	57.5	**0%**	2.51
OF.12	3.05	5	39.4	8.1	10.0	57.5	**5%**	2.51
OF.13	3.05	5	39.4	8.1	10.0	57.5	**10%**	2.51
OF.14	3.05	5	39.4	8.1	10.0	57.5	**20%**	2.51
OF.15	3.05	5	39.4	8.1	10.0	57.5	**30%**	2.51
OF.16	3.05	5	39.4	8.1	10.0	57.5	**60%**	2.51
OF.17	3.05	5	39.4	8.1	10.0	57.5	**80%**	2.51
OF.18	3.05	5	39.4	8.1	10.0	57.5	40%	**2.31**
OF.19	3.05	5	39.4	8.1	10.0	57.5	40%	**2.71**

(b) Classrooms

Case #	H (m)	n (ACH)	Q_{oz} /A (W/m^2)	Q_l /A (W/m^2)	Q_{ex} /A (W/m^2)	Q_t /A (W/m^2)	η (-)	h (m)
CL.1	**3.00**	4	15.1	8.1	5.0	28.2	40%	2.51
CL.2	**3.30**	4	15.1	8.1	5.0	28.2	40%	2.51
CL.3	**3.60**	4	15.1	8.1	5.0	28.2	40%	2.51
CL.4	3.30	**3**	15.1	8.1	5.0	28.2	40%	2.51
CL.5	3.30	**6**	15.1	8.1	5.0	28.2	40%	2.51
CL.6	3.30	4	**12.3**	**6.1**	**5.0**	**23.2**	40%	2.51
CL.7	3.30	4	**18.0**	**8.1**	**5.0**	**31.1**	40%	2.51
CL.8	3.30	4	**15.1**	**8.1**	**10.0**	**33.2**	40%	2.51
CL.9	3.30	4	**15.1**	**8.1**	**25.0**	**48.2**	40%	2.51
CL.10	3.30	4	15.1	8.1	5.0	28.2	**0%**	2.51
CL.11	3.30	4	15.1	8.1	5.0	28.2	**5%**	2.51

CL.12	3.30	4	15.1	8.1	5.0	28.2	**10%**	2.51
CL.13	3.30	4	15.1	8.1	5.0	28.2	**20%**	2.51
CL.14	3.30	4	15.1	8.1	5.0	28.2	**30%**	2.51
CL.15	3.30	4	15.1	8.1	5.0	28.2	**50%**	2.51
CL.16	3.30	4	15.1	8.1	5.0	28.2	40%	**2.31**
CL.17	3.30	4	15.1	8.1	5.0	28.2	40%	**2.81**

237

(c) Workshops

Case #	H (m)	n (ACH)	Q_{oz} /A (W/m^2)	Q_l /A (W/m^2)	Q_{ex} /A (W/m^2)	Q_t /A (W/m^2)	η (-)	h (m)
WS.1	**4.00**	4	34	8.1	10.0	52.1	40%	2.51
WS.2	**4.50**	4	34	8.1	10.0	52.1	40%	2.51
WS.3	**5.00**	4	34	8.1	10.0	52.1	40%	2.51
WS.4	4.50	4	**14.6**	**8.1**	**5.0**	**27.7**	40%	2.51
WS.5	4.50	4	**14.6**	**8.1**	**15.0**	**37.7**	40%	2.51
WS.6	4.50	4	**34.0**	**8.1**	**0.0**	**42.1**	40%	2.51
WS.7	4.50	4	**24.3**	**8.1**	**10.0**	**42.4**	40%	2.51
WS.8	4.50	4	**24.3**	**8.1**	**15.0**	**47.4**	40%	2.51
WS.9	4.50	4	34.0	8.1	10.0	52.1	**0%**	2.51
WS.10	4.50	4	34.0	8.1	10.0	52.1	**10%**	2.51
WS.11	4.50	4	34.0	8.1	10.0	52.1	**20%**	2.51
WS.12	4.50	4	34.0	8.1	10.0	52.1	**30%**	2.51
WS.13	4.50	4	34.0	8.1	10.0	52.1	**70%**	2.51
WS.14	4.50	**3**	34.0	8.1	10.0	52.1	40%	2.51
WS.15	4.50	**6**	34.0	8.1	10.0	52.1	40%	2.51
WS.16	4.50	4	34.0	8.1	10.0	52.1	40%	**2.70**
WS.17	4.50	4	34.0	8.1	10.0	52.1	40%	**3.00**

238
239

(d) Restaurants

Case #	H (m)	n (ACH)	Q_{oz} /A (W/m^2)	Q_l /A (W/m^2)	Q_{ex} /A (W/m^2)	Q_t /A (W/m^2)	η (-)	h (m)
RS.1	**3.00**	4	27.6	8.1	5.0	40.7	40%	2.51
RS.2	**3.30**	4	27.6	8.1	5.0	40.7	40%	2.51
RS.3	**3.60**	4	27.6	8.1	5.0	40.7	40%	2.51
RS.4	3.30	**3**	27.6	8.1	5.0	40.7	40%	2.51
RS.5	3.30	**7**	27.6	8.1	5.0	40.7	40%	2.51
RS.6	3.30	4	**21.0**	**8.1**	**5.0**	**34.1**	40%	2.51
RS.7	3.30	4	**30.0**	**6.0**	**0.0**	**36.0**	40%	2.51
RS.8	3.30	4	**30.0**	**9.6**	**0.0**	**39.6**	40%	2.51
RS.9	3.30	4	**30.0**	**9.6**	**5.0**	**44.6**	40%	2.51
RS.10	3.30	4	**25.4**	**9.6**	**25.0**	**60.0**	40%	2.51
RS.11	3.30	4	27.6	8.1	5.0	40.7	**0%**	2.51
RS.12	3.30	4	27.6	8.1	5.0	40.7	**10%**	2.51

RS.13	3.30	4	27.6	8.1	5.0	40.7	**20%**	2.51
RS.14	3.30	4	27.6	8.1	5.0	40.7	**30%**	2.51
RS.15	3.30	4	27.6	8.1	5.0	40.7	**50%**	2.51
RS.16	3.30	4	27.6	8.1	5.0	40.7	40%	**2.31**
RS.17	3.30	4	27.6	8.1	5.0	40.7	40%	**2.81**

Figs. 4 to 7 plot the temperature and contaminant concentration distributions in one representative from each indoor space. All the cases showed vertical temperature gradients. The contaminant concentrations could be stratified (e.g. Cases OF.8 and WS.10) or almost mixed (e.g. Cases CL.6 and RS.15), depending on their case specifications.

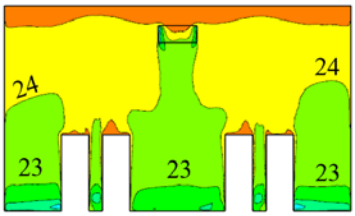

(a) Temperature distribution (°C)

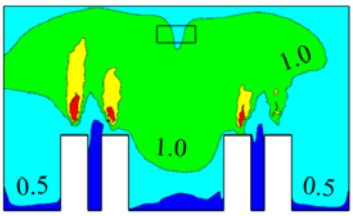

(b) Normalized contaminant concentration (C*)

Fig. 4 Results of Case OF.8

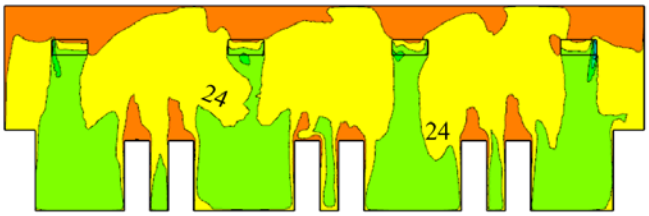

(a) Temperature distribution (°C)

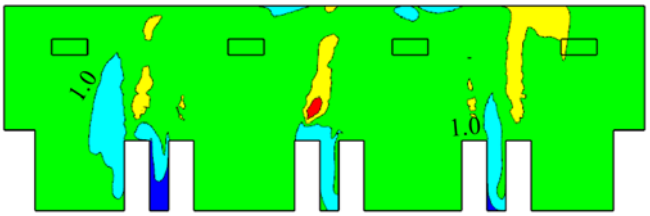

(b) Normalized contaminant concentration (C*)

Fig. 5 Results of Case CL.6

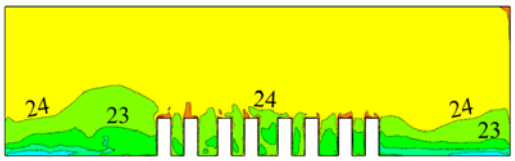

(a) Temperature distribution (°C)

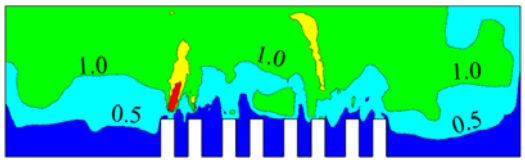

(b) Normalized contaminant concentration C*

Fig. 6 Results of Case WS.10

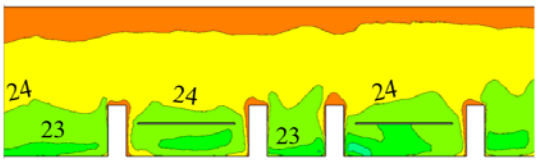

(a) Temperature distribution (°C)

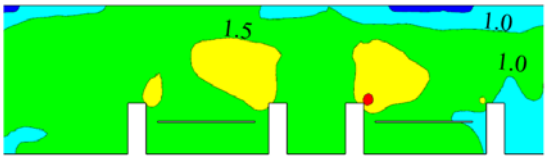

(b) Normalized contaminant concentration C*

Fig. 7 Results of Case RS.15

253

254 To explore the impacts of specific parameters have on temperature gradient and ventilation
255 effectiveness, it is essential to compare results from cases where only one parameter was changed.
256 Fig. 8 illustrates the ΔT_{ha} and VE results predicted by the CFD model for several typical cases:
257 OF.3, OF.4, OF.5, OF.11 and OF.17. These cases had different η and ACH, but the same values
258 for the other parameters. ΔT_{ha} represents the difference between averaged temperature at 1.1m and
259 that at 0.1m as defined in Section 2.3. Fig. 8(a) shows that at the same ACH, the ΔT_{ha} decreased
260 with η . This result verifies that the PCB effectively reduced the temperature gradient created by
261 DV. Meanwhile, at the same η , the ΔT_{ha} decreased with ACH. This occurred because an increase
262 in the airflow rate reduced the overall temperature difference ($T_e - T_s$) in the room and therefore
263 reduced ΔT_{ha} as well.

264 Next, Fig. 8 (b) displays the ventilation effectiveness predicted by CFD for these cases. Note that
265 the horizontal axis is VE_h , which is defined as $VE_h = (C_e - C_s)/(C_h - C_s)$ and C_h represents
266 average contaminant concentrations at various heights. Hence, VE_h was calculated to quantify the
267 air at different heights and was equal to VE when the sampling height was at head level of a sitting
268 occupant (1.1m). Since DV supplied clean air to the lower part of room and exhausted air near the
269 ceiling, VE_h was generally higher in the occupied zone than in the upper zone (mixing region).
270 Furthermore, since a PCB-induced jet recirculated the contaminant downward, a higher η led to a
271 lower VE. On the other hand, when η remained the same, VE increased with ACH, because an
272 increase in the supply airflow rate could increase the indoor airborne contaminant removal rate.
273 Hence, in a room with a DV-PCB system, VE is determined by the combined effects of airflow
274 supplied by the DV system and the downward jet induced by the PCB.

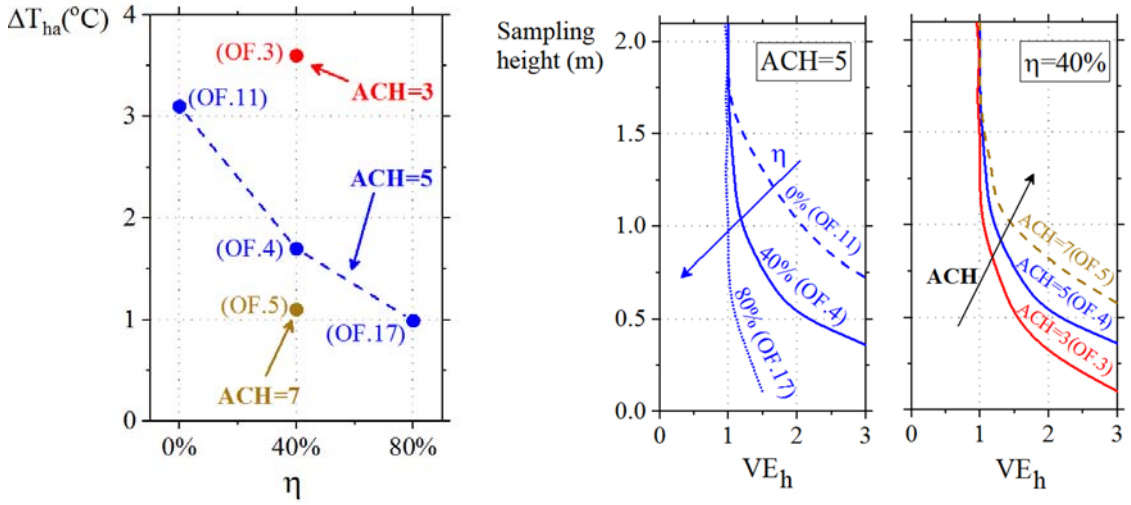

(a) ΔT_{ha} (b) Ventilation effectiveness

Fig. 8 ΔT_{ha} and ventilation effectiveness predicted by CFD model for several cases (contaminants released from the breathing level from the occupants)

The design parameters and boundary conditions listed in Table 2 along with the calculated ΔT_{ha} and VE results formed a database, which was used for model development as described in Section 3.2.

3.2 Mathematical models for ΔT_{ha} and VE

To quantify the thermal and ventilation performance of a DV-PCB system and to guide its design, we first correlated ΔT_{ha} with various design parameters by examining the airflow physics in a room with DV-PCB system, as shown in Section 2.4. With the established database, we had the values of all the independent variables $Q_{oz}/(\rho C_p nA)$, $Q_l/(\rho C_p nA)$, $Q_{ex}/(\rho C_p nA)$, $Q_{PCB}/(\rho C_p nA)$ as well as obtained the corresponding values of ΔT_{ha}. Through a regression analysis in Microsoft Excel [47], coefficients α_i and β in Eq. (8) were determined: $\alpha_{oz}=0.295, \alpha_l=0.132, \alpha_{ex}=0.185$ and $\beta=-0.203h_0/h$. Term h_0/h accounts for the influence of PCB height on β. When the height is infinitely large, the cooling effect of PCB on the occupied zone is negligible which makes $\beta \approx 0$. A typical PCB height of 2.6 m was used for h_0 [48]. Hence, the model for ΔT_{ha} can be expressed as:

$$\Delta T_{ha}=\frac{0.295Q_{oz}+0.132Q_l+0.185Q_{ex}-0.203\left(\frac{2.6}{h}\right)Q_{PCB}}{\rho C_p nA} \quad (9)$$

Eq. (9) indicates that different types of cooling loads contribute to ΔT_{ha} differently. Since Q_{oz} represents the cooling load in the occupied zone and has the most direct impact on ΔT_{ha}, α_{oz} is the largest among α_i. The Q_l is the load outside the occupied zone and has the smallest impact on ΔT_{ha}; thus, α_l is the smallest.

Next, this study developed a model for predicting ventilation effectiveness at breathing height (H = 1.1 m). Similarly, the coefficients in the mathematical expression were derived by the independent variables $Q_{oz}/(\rho C_p nA)$, $Q_l/(\rho C_p nA)$, $Q_{ex}/(\rho C_p nA)$, $Q_{PCB}/(\rho C_p nA)$ and obtained the corresponding VE. The model is expressed as:

$$VE = max\left\{2.83\left(1-e^{-n/3}\right)\frac{Q_{oz}+0.45Q_l+0.63Q_{ex}-0.79(2.6/h)(3.3/H)Q_{PCB}}{Q_t},\ 1\right\} \quad (10)$$

where the coefficients of Q_{oz}, Q_l and Q_{ex} are proportional to those in Eq. (9). Moreover, since air was supplied through DV diffusers at floor level and exhausted near the ceiling, once the contaminant concentration reached a mixed state at a certain height, it remained almost mixed at any height above. This characteristic is displayed in Fig. 8, and it was taken into account in Eq. (10). In this study, the ventilation effectiveness is with contaminants from the occupants, which are contaminant sources in indoor environments of many cases.

Figs. 9 and 10 plot the ΔT_{ha} and VE predicted by CFD and calculated by the mathematical models, namely, Eqs. (9) and (10). The coefficients in Eqs. (9) and (10) were determined by empirical fitting, which may partly explain the differences between the CFD results and the results of the models. In addition, numerical errors in the CFD simulations may have contributed to the discrepancies between the two sets of results. Nevertheless, the overall trends in ΔT_{ha} and VE were predicted with reasonably good accuracy for these cases. Compared with the CFD method, calculation using the mathematical models requires much less modeling and computational effort. The models could be easily used in the design process.

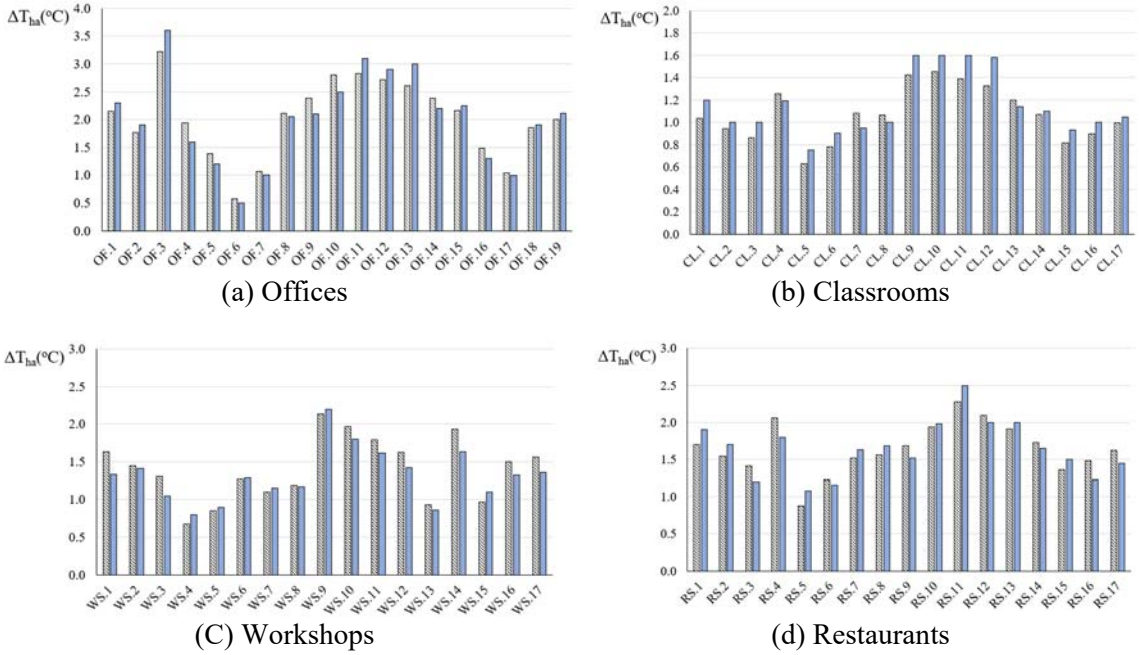

(a) Offices (b) Classrooms

(C) Workshops (d) Restaurants

Fig. 9 Comparison of ΔT_{ha} predicted by Eq. (9) and by CFD
(Standard error of regression: 0.19 K)

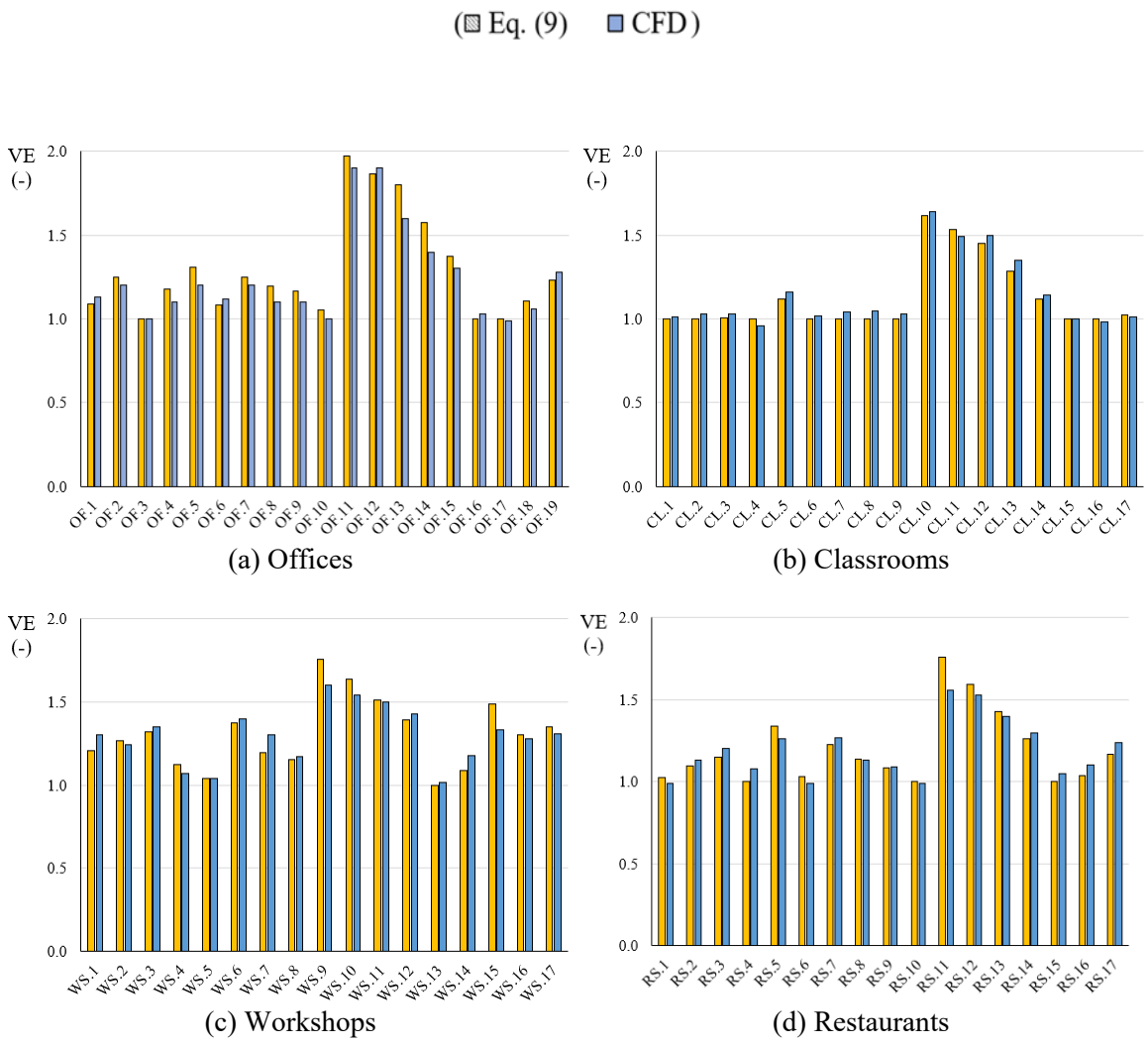

Fig. 10 Comparison of VE predicted by Eq. (10) and by CFD

3.3 Determination of η

According to Eqs. (9) and (10), which are described in Section 3.2, both ΔT_{ha} and VE are correlated with ACH and η, and thus the two equations are coupled. Plotting the ACH - η and VE - η relationships on the same graph provides a straightforward way of determining the optimal η for a DV-PCB system.

As an example, Fig. 11 shows the ACH - η and VE - η relationships generated from Eqs. (9) and (10) for the following parameters in an indoor space: Q_{oz} = 58 W/m^2, Q_l = 8 W/m^2, Q_{ex} = 5 W/m^2, workshop layout, H = 4.5 m, h = 2.51 m, and desired ΔT_{ha} = 3 K. The required ACH on the figure indicates the ACH needed to meet thermal comfort (ΔT_{ha}) requirement. Depending on the design target from a designer, the desired ΔT_{ha} could also be varied, and the curves on Fig. 11 would change accordingly. The two curves indicate that as η increases, ΔT_{ha} decreases, and thus the required ACH also decreases. Meanwhile, the increase in η causes a decrease in VE at breathing

level. In a design process, different η could be used. When a user selects a η, the required ACH and resultant VE can be found directly. In this case, for instance, $\eta = 40\%$ leads to VE = 1.2 and required ACH = 3.0.

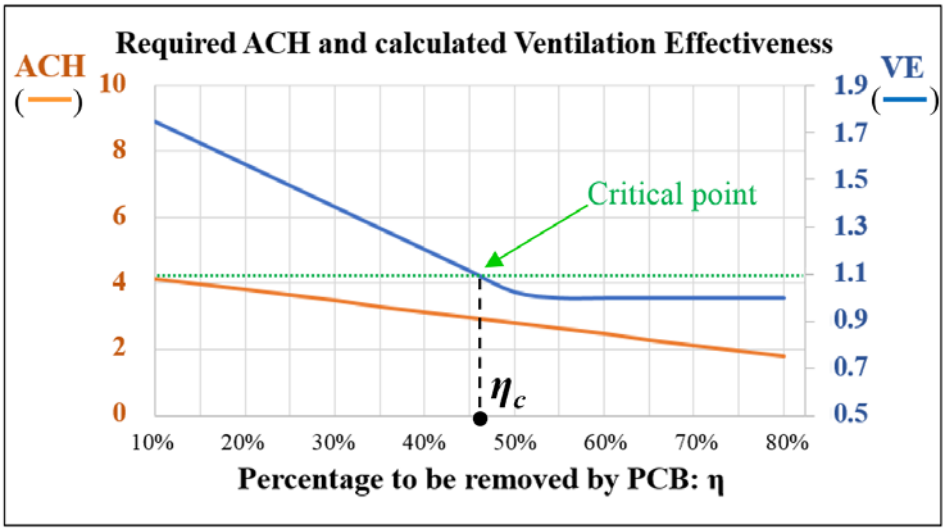

Fig. 11 ACH-η and VE-η relationships for a given set of indoor space specifications (Q_{oz} = 58 W/m^2, Q_l = 8 W/m^2, Q_{ex} = 5 W/m^2; workshop layout; H = 4.5 m, h = 2.51m)

This study recommends using a η that leads to VE > 1.1. Otherwise, the resulting air quality would be close to that in mixing mode ventilation, and the use of a DV-PCB system might not be economical. Therefore, Fig. 11 also includes a horizontal line at VE = 1.1, and its intersection with the VE-η curve is marked "critical point". In the design process, it is recommended that the designer select a η that is smaller than η_c.

After η has been selected for the DV-PCB system, the DV and PCB parts of the system can be designed separately.

3.4 Condensation control strategies for different air handling systems

Avoiding condensation on the surfaces of PCB coils is another important objective in the design of a DV-PCB system. Hence, this study evaluated the humidity in an indoor space with this coupled system, and proposed design strategies to prevent condensation from occurring.

Section 2.5 presented the two possible air handling systems for a DV-PCB design. Fig. 12 further illustrates four possible air handling processes on a psychrometric chart for each of the two systems. In relatively dry outdoor climates (processes 2 and 4), outdoor (or mixed) air is cooled and subsequently sent to indoor space. When outdoor air (or mixed air) has relatively high humidity ($\omega > \omega_D$), it must be dehumidified by a cooling coil, as shown in processes 1 and 3. Hence, the humidity of the supply air becomes:

$$\omega_I = min\left[\omega_D, \omega_M\right]$$

$$= min\left[\omega_D, x\omega_O + (1-x)\omega_E\right] \quad (11)$$

where x represents the proportion of outdoor air in mixed air. If the air system is a DOAS, $x = 1.0$ and $\omega > \omega_D$. Hence, Eq. (11) applies to both the DOAS and air recirculation system.

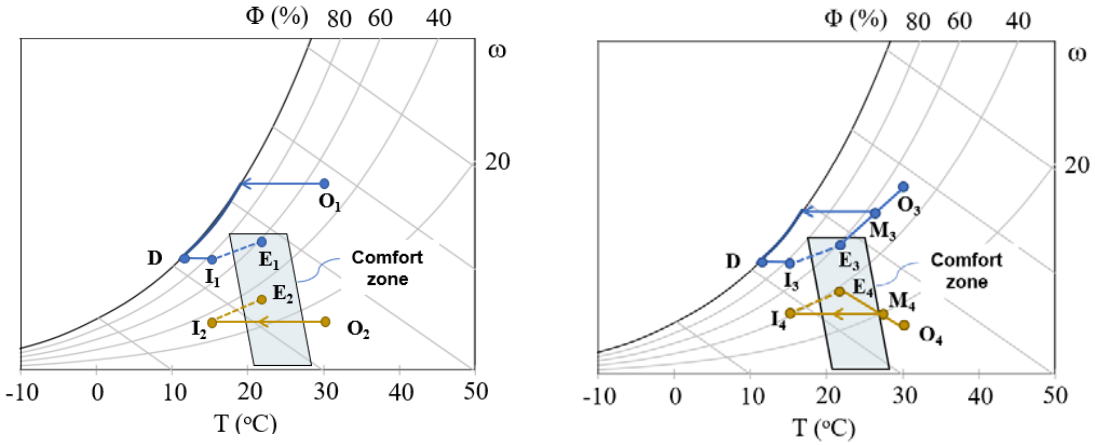

(a) DOAS (processes 1 and 2)

(b) Air recirculation system (processes 3 and 4)

Fig. 12 Air handling processes on psychrometric chart

Next, the humidity at the exhaust, ω_E, is calculated as:

$$\dot{m}_{air}\omega_E = \dot{m}_{air}\omega_I + S_{vapor} + \dot{m}_{inf}\omega_o \quad (12)$$

where $\dot{m}_{air}$ and $\dot{m}_{inf}$ ($\ll \dot{m}_{air}$) represent the mass flow rates of air from the HVAC system and through infiltration, respectively. The S_{vapor} stands for vapor generated inside the indoor space, which is mainly from occupants. According to TenWolde and Pilon [49], the average water vapor generation rate per person is $0.025\ g/s$.

Eq. (11) and Eq. (12) can be used to calculate ω_E which can be used in turn to obtain T_{dp-E}. To avoid condensation on the PCB coil surface, it is critical to ensure that PCB supply water temperature $T_{w,s} > T_{dp-E}$. After $T_{w,s}$ has been determined, a user can find the required chilled water flow rate on the data sheet provided in the corresponding PCB product manual.

3.5 Design guide and design interface

Based on the results obtained in the previous sections, this investigation proposed a step-by-step procedure for designing a DV-PCB system that provides satisfactory thermal comfort and indoor air quality. This procedure also eliminates the risk of condensation on the PCB cooling coil surface. Fig. 13 is a flowchart of the procedure.

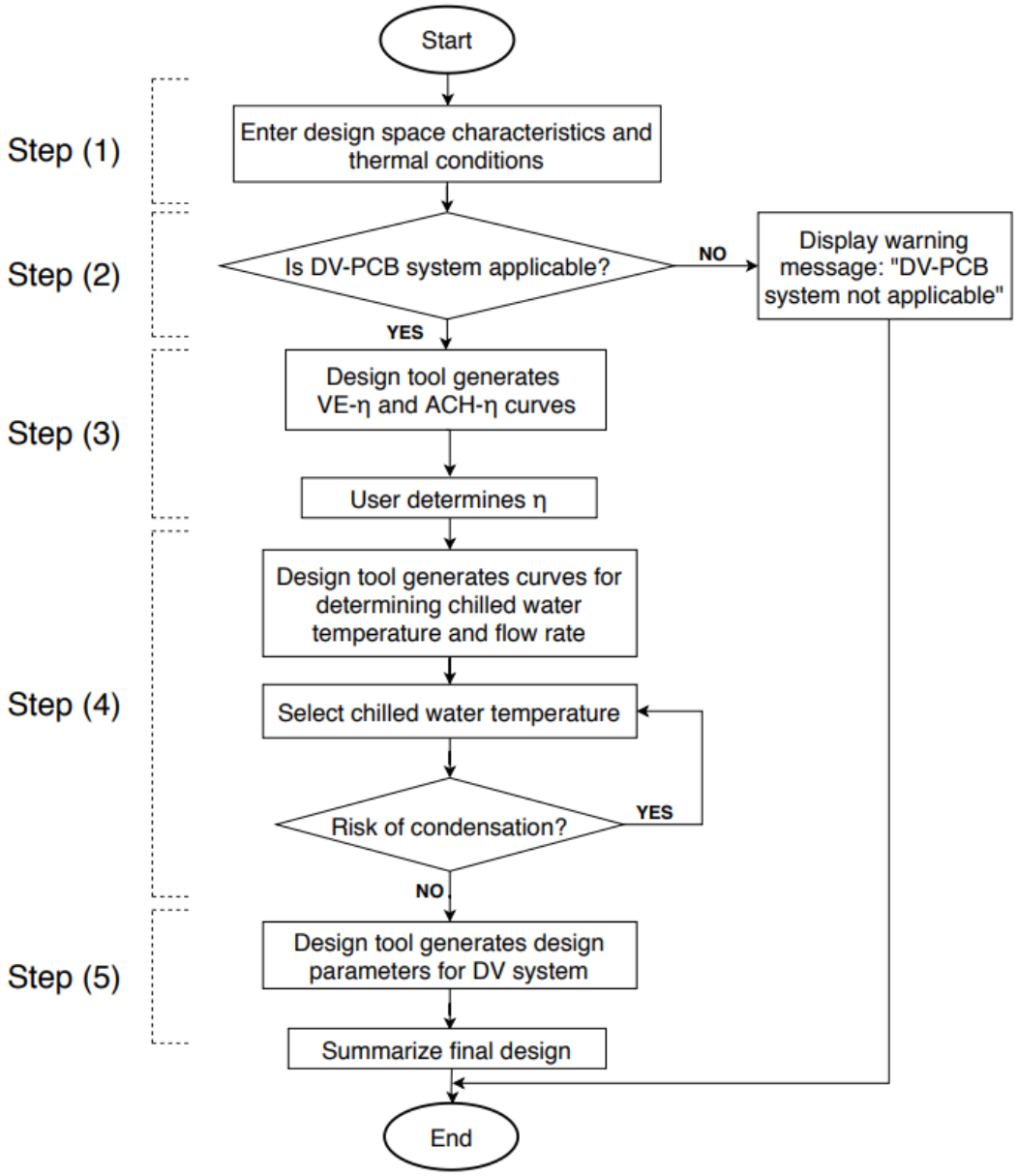

Fig. 13 Proposed procedure for designing DV-PCB system

The design process consists of five major steps, as follows.

(1) Obtain basic characteristics and thermal conditions of the indoor space for which the DV-PCB system is being designed. These include:

- Room dimensions: floor area and room height
- Type of indoor space: classroom, office, university laboratory, auditorium, etc.
- Cooling loads in the room in terms of Q_{oz}, Q_{ex} and Q_l.
- Required ΔT_{ha} and temperature setpoint T_{sp}.

(2) Assess the applicability of the system.

As previously mentioned, some studies have shown that a DV-only system may not be capable of providing thermal comfort in an indoor space with a cooling load larger than 40 W/m^2. However, for a cooling load smaller than 25 W/m^2, these studies all suggested that thermal comfort could be easily achieved by a DV-only system. Therefore, the design guide in the present study first rates the applicability of the DV-PCB system for an indoor space on the basis of its total cooling load Q_t: "Not needed" for $Q_t < 25$W/m^2, "Applicable" for 25 W/m^2 < $Q_t < 40$ W/m^2, and "Recommended" for $Q_t > 40$ W/m^2.

It is important that the PCB remove a significant percentage of the cooling load while still maintaining a satisfactory VE at breathing height, as indicated in Section 3.3. Hence, a DV-PCB is considered applicable only if $\eta_c > 15\%$ and it is recommended to select a η that makes resulting VE higher than 1.1. Otherwise the PCB is contributing too small portion of cooling or making indoor contaminant concentration close to a mixed condition, which makes the adoption of PCB non-economical.

(3) Determine η for the DV-PCB system.

The ACH-η and VE-η curves (shown in Fig. 11) are generated with the use of Eqs. (9) and (10). Designers can determine η for the coupled system. The value should be between 15% and η_c. The required ACH and resulting VE can then be obtained from the curves.

(4) Determine PCB design parameters.

The dewpoint temperature T_{dp-E} in the indoor space is calculated by Eqs. (11) and (12). To avoid condensation, the supply water temperature $T_{w,s}$ must be higher than T_{dp-E}. Designers can then find the required chilled water flow rate in the PCB product manual.

(5) Determine design parameters for the DV system.

Based on the ACH and VE calculated in Step (2), the required airflow rate V_h to maintain thermal comfort is:

$$V_h = \frac{ACH \cdot H \cdot A}{3600}$$

The required air flow rate V_f to meet the ventilation requirement is:

$$V_f = \frac{R_p \cdot N + R_A \cdot A}{VE}$$

Hence, the design flow rate is:

$$V = max\{V_h, V_f\}$$

Meanwhile, the supply air temperature is:

$$T_s = T_{sp} - \theta_f \frac{Q_t}{\rho C_p V}$$

and θ_f can be calculated by Mundt's formula [50].

Although the five-step guide provides a clear roadmap for designing a DV-PCB system, each step involves multiple calculations, and thus the process is time-consuming. To make the design process more convenient, this study further developed a design interface to automate and visualize the process. Once a designer enters the required inputs, the design interface automatically updates the

ACH-η and VE-η curves, displays the applicability rating of the DV-PCB system, and provides recommended design parameters.

3.6 Determination of required chilled water flow rate

Once the water supply temperature ($T_{w,s}$) has been selected, the required chilled water flow rate (q) for the PCB can be found in the corresponding product manual, as mentioned in Section 3.4. In the event that the manufacturer does not provide an easy-to-find table, a simple mathematical model can be used. European Committee for Standardization [51] used a regression model to correlate Q_{PCB} with the difference between room air temperature (T_{room}) and mean water temperature ($T_{w,m}$):

$$Q_{PCB} = k\left(T_{room} - T_{w,m}\right)^n \tag{13}$$

However, the mean water temperature cannot be easily determined. Furthermore, this model was based on one piece of PCB and does not account for variation in PCB size. In addition, Kim et al. [52] found that the chilled water flow rate (q) also affects Q_{PCB}. Hence, this study correlated Q_{PCB} with PCB cross-sectional area (WL), the difference between room air temperature and water supply temperature ($T_{room} - T_{w,s}$), and chilled water flow rate, as follows:

$$Q_{PCB} = k\left(WL\right)^m \left(T_{room} - T_{w,s}\right)^n q^l \tag{14}$$

By conducting multi-variable regression using 320 performance data points provided by TROX [53], this study obtained the following coefficients: $m = 1$, $n = 1.07$ and $l = 1.05$, as well as

$$k = 314.58 - 154.75W \tag{15}$$

The details of the multi-variable regression are provided in Appendix 1. Hence, Eq. (14) becomes:

$$Q_{PCB} = \left(314.58 - 154.75W\right)\left(WL\right)\left(T_{room} - T_{w,s}\right)^{1.07} q^{0.15} \tag{16}$$

In the market, the width of PCBs is usually standardized by the manufacturers, but the length can be customized according to design requirements. Therefore, it is more convenient to express Eq. (16) as the cooling capacity per unit length:

$$\frac{Q_{PCB}}{L} = \left(314.58 - 154.75W\right)W\left(T_{room} - T_{w,s}\right)^{1.07} q^{0.15} \tag{17}$$

Fig. 14 compares the calculated $\frac{Q_{PCB}}{L}$ with those from TROX [45]. The agreement between the two sets of results is good. Thus, Eq. (17) can be used to determine the required chilled water flow rate from $T_{w,s}$ and $\frac{Q_{PCB}}{L}$. Fig. 15 further shows the cooling capacity calculated by Eq. (17) for a PCB with W = 0.61 m, at different $\Delta T = \left(T_{room} - T_{w,s}\right)$. The curves clearly indicate that at the same

q and T_{room}, the cooling capacity significantly increases as $T_{w,s}$ decreases. They also show that the cooling capacity grows with q, although the growth rate decreases as q becomes larger.

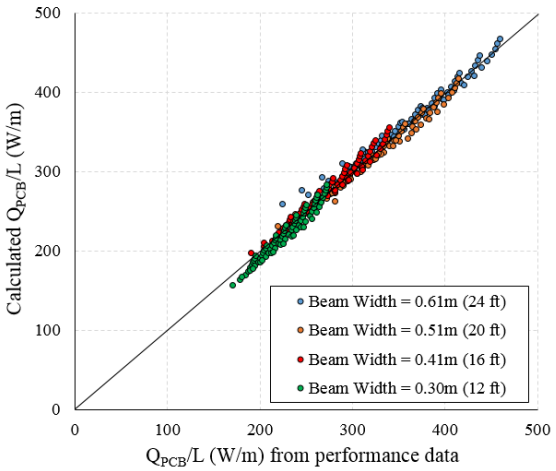

Fig. 14 Comparison of the calculated Q_{PCB}/L from Eq. (17) with the data from TROX [53]

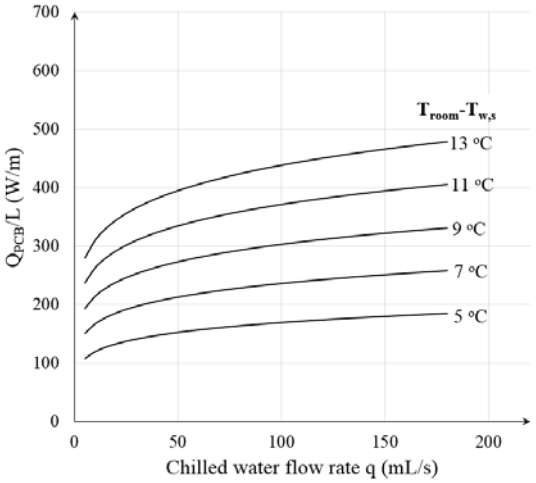

Fig. 15 PCB cooling capacity at different ΔT (beam width = 0.61 m)

Note that coefficients m, n and l in Eq. (14) are sensitive to the densities of the coils and fins inside the PCB. The coefficients in Eq. (17) are based on the data from TROX [53] and may be different for other PCBs. For a given PCB, one can use the multi-variable regression method in Appendix 1 to find the corresponding coefficients.

4. Discussion

4.1 Draft in DV-PCB system

The evaluation of thermal comfort provided by a DV-PCB system used the temperature gradient ΔT_{ha} as the criterion. This study did not consider other thermal comfort indices, such as the percentage dissatisfied due to draft (PD) [54], that have been used to appraise thermal comfort in many other studies [55, 56]. High PD (> 25%) could exist in the region directly below the PCB in an indoor space with a DV-PCB system, but the PD is relatively low (< 10%) in the bulk region of the room [24]. Therefore, in an indoor space with a DV-PCB system, it is not recommended that occupants sit right beneath the PCB. In the design of a room interior layout, if chairs are not placed right below PCB, the DV-PCB system designed using the proposed guide should lead to very low risk of draft to occupants.

4.2 Limitations

The calculation of indoor humidity assumed that the air handling system used in DV-PCB was either a DOAS or an air recirculation system. Although these two configurations are the most common and least costly, other variations are possible. For example, one could use a heat recovery

system [57] in which a portion of the return air is utilized to cool or heat outdoor air through the heat exchanger, but the return air does not mix with outdoor air. More recent technologies, such as desiccant wheels [58], can also be incorporated into the air handling unit to improve energy efficiency, although they will increase the first cost of the HVAC system. If these variations are used for the air system, the air-handling process could differ from those shown in Fig. 12, and Eq. (12) should be adjusted accordingly. However, all other equations and associated design steps will remain unchanged.

This investigation mainly studied the thermal and ventilation performance of a DV-PCB system, and proposed design guidelines accordingly. For comprehensive evaluation of a system, it is also important to examine its energy and economic performance, and the DV-PCB should be compared with conventional DV-only or mixing ventilation systems in terms of these two aspects. The results would provide more complete information about the market value and potential of DV-PCB system. This was not within the scope of the present study but deserves further attention.

5. Conclusions

This research systematically investigated the impact of PCB on the thermal and ventilation performance of a DV system. The heat transfer characteristics and airflow distributions in a DV-PCB system were very different from those in a coupled DV and chilled ceiling system. Proper selection of design parameters is essential to ensure the thermal comfort and indoor air quality requirements could be satisfied. With an established database of 70 cases, this study further developed a guideline for designing a coupled DV-PCB system which meets thermal and ventilation needs of a room while avoiding condensation risk. The research led to the following conclusions:

(1) The ΔT_{ha} in a DV-PCB system was positively related to the cooling loads in the room and negatively related to ACH and η. With the results from the database, a mathematical model was developed to calculate ΔT_{ha}.

(2) The same database was used to develop a model for calculating ventilation effectiveness at breathing height in a DV-PCB system. At the same height in the room, ventilation effectiveness increased with ACH but decreased with η.

(3) This research established a strategy to avoid condensation on the PCB cooling coil surface by controlling the PCB supply water temperature in accordance with the estimated indoor dewpoint temperature. A method was developed for obtaining the required chilled water flow rate from the PCB supply water temperature.

(4) With the ΔT_{ha} and VE models developed here, ACH-η and VE-η curves can be generated to determine the maximum η that can be used in a DV-PCB system. Based on these curves and other results, this study developed a five-step procedure for designing a DV-PCB system. A DV-PCB

system designed in accordance with this guide will provide satisfactory thermal comfort and air quality without the risk of condensation.

Acknowledgement

This research was partially sponsored by the American Society of Heating, Refrigerating and Air-conditioning Engineers (ASHRAE) through research project 1666.

References

[1] Lin, Z., Chow, T. T., Fong, K. F., Tsang, C. F., & Wang, Q. (2005). Comparison of performances of displacement and mixing ventilations. Part II: Indoor air quality. International Journal of Refrigeration, 28(2), 288-305.

[2] Norbäck, D., Wieslander, G., Zhang, X., & Zhao, Z. (2011). Respiratory symptoms, perceived air quality and physiological signs in elementary school pupils in relation to displacement and mixing ventilation system: An intervention study. Indoor Air, 21(5), 427-437.

[3] Lin, Z., Lee, C. K., Fong, S., Chow, T. T., Yao, T., & Chan, A. L. S. (2011). Comparison of annual energy performances with different ventilation methods for cooling. Energy and Buildings, 43(1), 130-136.

[4] Burt, L. W. (2007). Life cycle cost of displacement ventilation in an office building with a hot and humid climate (Doctoral dissertation, University of Florida).

[5] Mateus, N. M., & da Graça, G. C. (2015). A validated three-node model for displacement ventilation. Building and Environment, 84, 50-59.

[6] Rees, S. J., & Haves, P. (2013). An experimental study of air flow and temperature distribution in a room with displacement ventilation and a chilled ceiling. Building and Environment, 59, 358-368.

[7] Alain, M., Kamel, G., & Nesreen, G. (2012). A simplified combined displacement and personalized ventilation model. HVAC&R Research, 18(4), 737-749.

[8] Cho, Y., Awbi, H. B., & Karimipanah, T. (2005, September). Comparison between wall confluent jets and displacement ventilation in aspect of the spreading ratio on the floor. In Proceedings of the 10th International Conference in Indoor Air Quality and Climate, Beijing, China (pp. 4-9).

[9] Yuan, X., Chen, Q., & Glicksman, L. R. (1998). A critical review of displacement ventilation. ASHRAE Transactions, 104, 78-90.

[10] Olesen, B. W., Koganei, M., Holbrook, G. T., & Woods, J. E. (1994). Evaluation of a vertical displacement ventilation system. Building and Environment, 29(3), 303-310.

[11] Ghaddar, N., Ghali, K., & Saadeh, R. (2010). Optimized selection and operation of the combined chilled ceiling system and displacement ventilation. International Journal of Energy Research, 34(15), 1328-1340.

[12] Schiavon, S., Bauman, F., Tully, B., & Rimmer, J. (2012). Room air stratification in combined chilled ceiling and displacement ventilation systems. HVAC&R Research, 18(1-2), 147-159.

[13] Chakroun, W., Ghaddar, N., & Ghali, K. (2011). Chilled ceiling and displacement ventilation aided with personalized evaporative cooler. Energy and Buildings, 43(11), 3250-3257.

[14] Ghali, K., Ghaddar, N., & Ayoub, M. (2007). Chilled ceiling and displacement ventilation system for energy savings: A case study. International Journal of Energy Research, 31(8), 743-759.

[15] Bahman, A., Chakroun, W., & Saade, R. (2009). Performance comparison of conventional and chilled ceiling/displacement ventilation systems in Kuwait. ASHRAE Transactions, 115, 587.

[16] Novoselac, A., & Srebric, J. (2002). A critical review on the performance and design of combined cooled ceiling and displacement ventilation systems. Energy and buildings, 34(5), 497-509.

[17] Yin, Y., Zhang, X., and Chen, Q. 2009. "Condensation risk in a room with high latent load and chilled ceiling panel and with air supplied from liquid desiccant system," HVAC&R Research, 15(2): 315-327.

[18] Weidner, S., Doerger, J., & Walsh, M. (2009). Cooling with less air: Using underfloor air distribution and chilled beams. ASHRAE Journal, 51(12), 34-41.

[19] Mumma, S. A. (2001). Ceiling panel cooling systems. ASHRAE Journal, 43(11), 28-32.

[20] Kosonen, R., Saarinen, P., Koskela, H., & Hole, A. (2010). Impact of heat load location and strength on air flow pattern with a passive chilled beam system. Energy and Buildings, 42(1), 34-42.

[21] Roth, K., Dieckmann, J., Zogg, R., & Brodrick, J. (2007). Chilled beam cooling. ASHRAE Journal, 49(9), 84.

[22] Nelson, I. (2012). The effect of thermal load configurations on passive chilled beam performance. Ph.D. dissertation. Department of Mechanical Engineering, Texas A&M University, College Station, TX.

[23] Fredriksson, J., & Sandberg, M. (2009). The effect of false ceiling on the cooling capacity of passive chilled beams. Building and Environment, 44(7), 1426-1430.

[24] Shi, Z., Lu, Z., & Chen, Q. (2019). Indoor airflow and contaminant transport in a room with coupled displacement ventilation and passive-chilled-beam systems. Building and Environment, 106244.

571 [25] Fredriksson, J., Sandberg, M., & Moshfegh, B. (2001). Experimental investigation of the
572 velocity field and airflow pattern generated by cooling ceiling beams. Building and environment,
573 36(7), 891-899.

574 [26] Shan, W., & Rim, D. (2018). Thermal and ventilation performance of combined passive
575 chilled beam and displacement ventilation systems. Energy and Buildings, 158, 466-475.

576 [27] Keblawi, A., Ghaddar, N., Ghali, K., & Jensen, L. (2009). Chilled ceiling displacement
577 ventilation design charts correlations to employ in optimized system operation for feasible load
578 ranges. Energy and Buildings, 41(11), 1155-1164.

579 [28] Ge, G., Xiao, F., & Wang, S. (2012). Neural network based prediction method for preventing
580 condensation in chilled ceiling systems. Energy and Buildings, 45, 290-298.

581 [29] Kim, M. K., & Leibundgut, H. (2014). Advanced airbox cooling and dehumidification system
582 connected with a chilled ceiling panel in series adapted to hot and humid climates. Energy and
583 Buildings, 85, 72-78.

584 [30] Mumma, S. A. (2003). Chilled ceiling condensation control. ASHRAE IAQ
585 Applications, 4(4), 22-23.

586 [31] Brennan, T., & Burge, H. (2005). Assessing mold in buildings. ASHRAE Journal, 47(1),
587 S158.

588 [32] Lee, K. (2009). Air distribution effectiveness with stratified air distribution
589 systems. ASHRAE Transactions, 115, 322.

590 [33] Gilani, S., Montazeri, H., & Blocken, B. (2016). CFD simulation of stratified indoor
591 environment in displacement ventilation: Validation and sensitivity analysis. Building and
592 Environment, 95, 299-313.

593 [34] Pianta, R. C., Belsky, J., Houts, R., & Morrison, F. (2007). Opportunities to learn in America's
594 elementary classrooms. Science, 315(5820), 1795-1796.

595 [35] National Center for Education Statistics (NCES). 2011. Highest degree earned, years of full-
596 time teaching experience, and average class size for teachers in public elementary and secondary
597 schools, by state: 2011-12. Retrieved June 2018 from: https://nces.ed.gov/programs/
598 digest/d14/tables/dt14_209.30.asp?current=yes

599 [36] New York State Department of Health (DOH). (2010). Retrieve May 2018 from:
600 https://www.health.ny.gov/professionals/ems/education/course_sponsors/docs/classroom_design_
601 standards.pdf

602 [37] U.S. General Service Administration. (2018). Retrieved April 2018 from:
603 https://www.gsa.gov/ node/82314

[38] Hu, S., Chen, Q., & Glicksman, L. R. (1999). Comparison of energy consumption between displacement and mixing ventilation systems for different US buildings and climates. ASHRAE Transactions, 105, 453-464.

[39] National Optical Astronomy Observatory (NOAO). 2015. Retrieved May 2018 from: https://www.noao.edu/education/QLTkit/ACTIVITY_Documents/Safety/LightLevels_outdoor+indoor.pdf

[40] Handbook-Fundamentals, ASHRAE. (2009). Non-residential cooling and heating load calculations. American Society of Heating, Refrigerating and Air Conditioning Engineers.

[41] Standard, ASHRAE. (2010). Standard 55-2010, Thermal environmental conditions for human occupancy. American Society of Heating, Refrigerating and Air Conditioning Engineers.

[42] Standard, ASHRAE. (2013). Standard 62.1-2010, Ventilation for acceptable indoor air quality. American Society of Heating, Refrigerating and Air Conditioning Engineers.

[43] Fredriksson, J., & Sandberg, M. (2009). The effect of false ceiling on the cooling capacity of passive chilled beams. Building and Environment, 44(7), 1426-1430.

[44] Yakhot, V., Orszag, S. A., Thangam, S., Gatski, T. B., & Speziale, C. G. (1992). Development of turbulence models for shear flows by a double expansion technique. Physics of Fluids A: Fluid Dynamics, 4(7), 1510-1520.

[45] Zhang, Z., Zhang, W., Zhai, Z. J., & Chen, Q. Y. (2007). Evaluation of various turbulence models in predicting airflow and turbulence in enclosed environments by CFD: Part 2—Comparison with experimental data from literature. HVAC&R Research, 13(6), 871-886.

[46] ANSYS Inc. (2016). ANSYS Fluent Theory Guide 17.0, Canonsburg, PA.

[47] Microsoft Corporation. (2016). Microsoft Excel. Retrieved 2018 from: https://www.microsoft.com/en-us/

[48] Archtoolbox. (2018). Chilled beams and chilled ceilings. Retrieved 2018 from: https://www.archtoolbox.com/materials-systems/hvac/chilled-beam-ceiling.html

[49] TenWolde, A., & Pilon, C. L. (2007). The effect of indoor humidity on water vapor release in homes. In Proceedings, Thermal Performance of the Exterior Envelopes of Whole Buildings X. Atlanta, GA: American Society of Heating, Refrigerating and Air-Conditioning Engineers, Inc.

[50] Mundt, E. (1995). Displacement ventilation systems—Convection flows and temperature gradients. Building and Environment, 30(1), 129-133.

[51] European Committee for Standardization. (2005). Ventilation for buildings. Chilled beams. Testing and rating of passive chilled beams. BSEN 14518: 2005.

[52] Kim, J., Tzempelikos, A., Horton, W. T., & Braun, J. E. (2018). Experimental investigation and data-driven regression models for performance characterization of single and multiple passive chilled beam systems. Energy and Buildings, 158, 1736-1750.

[53] TROX Technik. (2017). Passive chilled beams, Type PKV. Retrieved November 20, 2017, from https://www.trox.de/en/passive-chilled-beam/type-pkv-c1247d25a7110473

[54] Fanger, P. O., Melikov, A. K., Hanzawa, H., & Ring, J. (1989). Turbulence and draft. ASHRAE Journal, (April), 18-25.

[55] Wang, Y., Lian, Z., Broede, P., & Lan, L. (2012). A time-dependent model evaluating draft in indoor environment. Energy and Buildings, 49, 466-470.

[56] Volkov, A. A., Sedov, A. V., & Chelyshkov, P. D. (2014). Modelling the thermal comfort of internal building spaces in social buildings. Procedia Engineering, 91, 362-367.

[57] Nasif, M., Al-Waked, R., Morrison, G., & Behnia, M. (2010). Membrane heat exchanger in HVAC energy recovery systems, systems energy analysis. Energy and Buildings, 42(10), 1833-1840.

[58] Kim, J., Tzempelikos, A., & Braun, J. E. (2019). Energy savings potential of passive chilled beams vs air systems in various US climatic zones with different system configurations. Energy and Buildings, 186, 244-260.

Appendix 1: MATLAB code for obtaining coefficients in Eq. (17)

```
%Read data points

q1 = xlsread('PCB_Cooling_Data.xlsx', 1, 'B2:B81');
q2 = xlsread('PCB_Cooling_Data.xlsx', 1, 'B83:B162');
q3 = xlsread('PCB_Cooling_Data.xlsx', 1, 'B165:B244');
q4 = xlsread('PCB_Cooling_Data.xlsx', 1, 'B248:B327');

Delta_T1 = xlsread('PCB_Cooling_Data.xlsx', 1, 'C2:C81');
Delta_T2 = xlsread('PCB_Cooling_Data.xlsx', 1, 'C83:C162');
Delta_T3 = xlsread('PCB_Cooling_Data.xlsx', 1, 'C165:C244');
Delta_T4 = xlsread('PCB_Cooling_Data.xlsx', 1, 'C248:C327');

Q1 = xlsread('PCB_Cooling_Data.xlsx', 1, 'E2:E81');
Q2 = xlsread('PCB_Cooling_Data.xlsx', 1, 'E83:E162');
Q3 = xlsread('PCB_Cooling_Data.xlsx', 1, 'E165:E244');
Q4 = xlsread('PCB_Cooling_Data.xlsx', 1, 'E248:E327');

ln_q1 = log(q1);
ln_q2 = log(q2);
ln_q3 = log(q3);
ln_q4 = log(q4);

ln_Delta_T1 = log(Delta_T1);
ln_Delta_T2 = log(Delta_T2);
ln_Delta_T3 = log(Delta_T3);
ln_Delta_T4 = log(Delta_T4);

ln_Q1 = log(Q1);
ln_Q2 = log(Q2);
ln_Q3 = log(Q3);
ln_Q4 = log(Q4);

X1 = [ones(size(ln_q1)) ln_q1 ln_Delta_T1];
b1 = regress (ln_Q1, X1);
```

```
X2 = [ones(size(ln_q2)) ln_q2 ln_Delta_T2];
b2 = regress (ln_Q2, X2);

X3 = [ones(size(ln_q3)) ln_q3 ln_Delta_T3];
b3 = regress (ln_Q3, X3);

X4 = [ones(size(ln_q4)) ln_q4 ln_Delta_T4];
b4 = regress (ln_Q4, X4);

n = mean([b1(3) b2(3) b3(3) b4(3)]);
l = mean([b1(2) b2(2) b3(2) b4(2)]);

W = [0.6096; 0.508; 0.4064; 0.3048]
K = exp([mean(ln_Q1 - l*ln_q1 - n*ln_Delta_T1);
    mean(ln_Q2 - l*ln_q2 - n*ln_Delta_T2);
    mean(ln_Q3 - l*ln_q3 - n*ln_Delta_T3);
    mean(ln_Q4 - l*ln_q4 - n*ln_Delta_T4)])
p = polyfit(W,K,1)
```

656